# Effect of Static Preloading on the Dynamic Stability of Structures

George J. Simitses*
*Georgia Institute of Technology, Atlanta, Georgia*

**The paper discusses the dynamic stability of statically preloaded structural configurations. Concepts of dynamic stability are presented, including criteria and estimates of critical conditions. These, then, are demonstrated through 1) a simple mechanical model, 2) a transversely loaded shallow arch, and 3) an axially loaded, geometrically imperfect, thin, circular, cylindrical shell.**

## Nomenclature

*General and Model*

$e, \bar{e}$ = load eccentricity for the model ($\bar{e} = e/L$)
$I$ = model moment of inertia about point A
$k$ = model spring stiffness
$L$ = model length or system position
$L_S^{P_0}$ = (near) stable static equilibrium position
$L_u^{P_0}$ = unstable static equilibrium position
$\bar{U}_T^M$ = modified total potential expression
$\bar{U}_T^{P_0}$ = total potential corresponding to static preloading
$\bar{U}_T^{P_0+P}$ = total potential corresponding to total load (static + dynamic)
$\theta$ = model degree of freedom (angle)
$\tau_0$ = nondimensionalized, load duration, time parameter
$\tau$ = model nondimensionalized time parameter ($\sqrt{ka^2/I}$)

*Arch Problem*

$a_i$ = see Eq. (20)
$e$ = arch rise parameter, Eq. (19)
$L$ = arch length
$\bar{p}$ = nondimensionalized axial force parameter
$p$ = nondimensionalized transverse force parameter, $= q_1 + e$
$P_E$ = Euler load
$q$ = nondimensionalized transverse force parameter, $\rho Q^*/P_E \epsilon_E L$
$P_E$ = Euler load for columns of length $L$
$Q^*$ = transverse load, Fig. 4
$r$ = $a_1 + e$
$u(x)$ = arch in-plane displacement component
$v(\xi)$ = nondimensionalized in-plane displacement component
$w_0(x)$ = undeformed arch shape function, Fig. 4
$w(x)$ = deformed arch shape function (transverse displacement = $w$-$w_0$)
$x$ = arch coordinate
$\epsilon_E$ = Euler strain; $(\pi\rho/L)^2$
$\eta(\xi)$ = nondimensionalized deformed arch shape function, $= w/\rho$
$\xi$ = $\pi x/L$
$\rho$ = radius of gyration for arch cross section
$\sigma$ = arch mass density (per unit volume)
$\tau$ = nondimensionalized time parameter

*Shell Problem*

$E$ = Young's modulus of elasticity for shell material
$h$ = shell wall thickness
$i, k, l$ = wavenumbers Eq. (29)
$P$ = applied stress
$\bar{p}$ = nondimensionalized applied stress, $= PR/Eh$
$\bar{U}_{T\ \mathrm{mod}}^P$ = $\bar{U}_T^P - (1-\nu^2)\bar{p}^2$
$\bar{U}_T^P$ = total potential expression
$u, v$ = in-plane displacement components
$u_p, v_p$ = particular solution for displacement components
$w$ = transverse displacement component
$\bar{w}$ = initial geometric imperfection, Eq. (30)
$\lambda_s$ = critical (static) load parameter, $= P_{\mathrm{cr}}/\sigma_{\mathrm{cl}}$
$\nu$ = Poisson's ratio (shell material)
$\xi_i$ = see Eq. (29)
$\bar{\xi}_i$ = see Eq. (30)
$\sigma_{\mathrm{cl}}$ = classical critical stress (static)

## Introduction

THE term "dynamic stability" encompasses several classes of problems and has been used, by various investigators, in connection with a particular study. Examples of these include problems of parametric excitation,[1] "follower force" type problems,[2,3] problems of aeroelastic stability, and others.[4-8]

A large class of structural problems that has received attention recently is that of impulsively loaded systems, as well as suddenly loaded systems with constant loads of infinite duration.[9-20] The systems considered in Refs. 9-20 are subject to either limit point instability or unstable bifurcation instability when loaded quasistatically. Furthermore, the external and internal loads are conservative and, therefore, these systems are conservative. A few solutions have appeared in the literature dealing with these types of systems, when loaded suddenly with a constant load of finite duration.[21,22]

This paper deals with systems (of this latter category) which are first loaded quasistatically to a level below the static critical load, and, subsequently, are subjected to sudden loads of constant magnitude and finite duration. Clear concepts of dynamic stability or instability are presented including criteria and estimates for critical conditions. These are demonstrated through several systems, including 1) a simple mechanical model, which is typical of an imperfection-sensitive structural configuration, 2) a laterally loaded shallow arch (similar in geometry to the one treated in Refs. 9, 12, and 14), and 3) an imperfect thin cylindrical shell (the same as the one treated in Ref. 20) loaded by axial compression.

In all of the reported investigations of suddenly loaded structures, it is assumed that the system is free of loading and that a step load is suddenly applied for a given time duration (including the extreme cases). A lot of insight and knowledge was gained from these studies. The present investigation deals with the more realistic case, in which the structure is first loaded quasistatically and then is subjected to a dynamic load. Consider, for example, a submarine resting at the bottom of the ocean (static preloading) subjected to a sudden blast loading (depth charge). The precise statement of the problem is given next.

Presented as Paper 82-0692 at the AIAA/ASME/ASCE/AHS 23rd Structures, Structural Dynamics and Materials Conference, New Orleans, La., May 10-12, 1982; submitted May 12, 1982; revision received Oct. 26, 1982. 

*Professor of Engineering Science and Mechanics. Associate Fellow AIAA.

Consider a structural configuration at its stable equilibrium position $L_S^{P_0}$, when subjected to an initial static load $P_0$. At time $t=0$, an additional constant load $P$ is suddenly applied to the system and acts only for a finite duration time $t=T_0$. After the release of the force $P$, the system moves because of the acquired total energy during the action of the load $P$. The system will be called dynamically stable if its motion is "unbuckled," meaning that its motion is bounded.[12] Since the systems under consideration exhibit limit or unstable bifurcation point instability, the system is stable if the energy, imparted through the action of the load $P$, is insufficient for the system to reach the unstable static equilibrium point on the "$P_0$-load" total potential of the system with zero velocity (zero kinetic energy). For each individual system, the criterion is invoked and estimates for critical conditions are found. The extreme cases of $T_0\to\infty$ (constant load of infinite duration) and $T_0\to 0$ (ideal impulse) are treated as special cases.

## Concepts and General Procedure

The concept of dynamic stability and the general procedures are extensions of those developed for the case of suddenly loaded systems without preloading.[22] The static equilibrium positions of the preloaded system are given as solutions to

$$\frac{\partial \bar{U}_T^{P_0}(L)}{\partial L}=0 \tag{1}$$

where $\bar{U}_T^{P_0}$ is the total potential and $L$ the position of the system. Thus, one may find all the $P_0$-load static equilibrium positions including the near stable position $L_S^{P_0}$ and the unstable position $L_u^{P_0}$, through which dynamic instability can be realized (see Fig. 1).

The concept of dynamic instability is next explained through the use of Fig. 1, which holds for one-degree-of-freedom systems, but the explanation is applicable to all finite-degree-of-freedom systems.

The system is initially loaded quasistatically by load $P_0$ and it reaches point A ($L=L_S^{P_0}$; stable static equilibrium point). Then, a load $P$ is applied suddenly for a time $\tau_0$ (finite duration). At $\tau_0$ the load $P$ is removed and the system has reached a position $L_{\tau_0}^{P_0+P}$.

A potential $\bar{U}_T^M$ is defined, such that $\bar{U}_T^M=\bar{U}_T^{P_0}$ at $\tau=0$ orat $L=L_S$ (see Fig. 1).

$$\bar{U}_T^M=\bar{U}_T^{P_0+P}+[\bar{U}_T^{P_0+P}(L_S^{P_0})-\bar{U}_T^{P_0+P}(L_S^{P_0})] \tag{2}$$

Since the system is conservative, during the action of $P$, one may write

$$\bar{U}_T^M+\bar{T}^{P_0+P}=\bar{U}_T^{P_0}(L_S^{P_0}); \qquad 0<\tau\le\tau_0 \tag{3}$$

where $\bar{T}^{P_0+P}$ is the kinetic energy of the system. Making use of Eq. (2), Eq. (3) becomes

$$\bar{U}_T^{P_0+P}+\bar{T}^{P_0+P}=\bar{U}_T^{P_0+P}(L_S^{P_0}); \qquad 0<\tau\le\tau_0 \tag{4}$$

For times greater than $\tau_0$, the system is also conservative and conservation of energy yields

$$\bar{U}_T^{P_0}+\bar{T}^{P_0}=\bar{U}_T^{P_0}(\tau_0)+\bar{T}^{P_0}(\tau_0); \qquad \tau>\tau_0 \tag{5}$$

If the force $P$ has imparted sufficient energy into the systems, such that it can reach the unstable point B ($L=L_u^{P_0}$; see Fig. 1) on the $P$-load potential with zero kinetic energy (velocity), then buckled motion is possible, and the system becomes dynamically unstable.

Note that the potential $\bar{U}_T^M$ does not enter the computations. It is only defined and shown on Fig. 1 in order to explain the extension of the previously developed concepts[12,22] for zero static preloading to the present case. It is clearly seen from Fig. 1 that if the origin of the system of axes ($\bar{U}_T$ and $L$) is moved to point A, then the role of $\bar{U}_T^0$ (zero-load total potential) is played by $\bar{U}_T^{P_0}$ and the role of $\bar{U}_T^P$ by $\bar{U}_T^M$.

The governing equations of predicting critical conditions are obtained from Eqs. (4) and (5). By requiring kinematic continuity at $\tau=\tau_0$ one may write

$$\bar{T}^{P_0+P}(\tau_0)=\bar{T}^{P_0}(\tau_0) \tag{6}$$

From Eq. (4) one may write

$$\bar{T}^{P_0+P}(\tau_0)=\bar{U}_T^{P_0+P}(L_S^{P_0})-\bar{U}_T^{P_0+P}(\tau_0) \tag{7}$$

Substitution of Eqs. (6) and (7) into Eq. (5) yields

$$\bar{U}_T^{P_0}+\bar{T}^{P_0}=\bar{U}_T^{P_0}(\tau_0)-\bar{U}_T^{P_0+P}(\tau_0)+\bar{U}_T^{P_0+P}(L_S^{P_0}); \text{ for } \tau>\tau_0 \tag{8}$$

A critical condition exists if the system can reach point B (see Fig. 1) with zero kinetic energy [$\bar{T}^{P_0}(L_u^{P_0})=0$]; by denoting the critical condition by ($P,\tau_{0_{cr}}$), one may write

$$\bar{U}_T^{P_0}(L_u^{P_0})=\bar{U}_T^{P_0}(\tau_{0_{cr}})-\bar{U}_T^{P_0}(\tau_{0_{cr}})+\bar{U}_T^{P_0+P}(L_S^{P_0}) \tag{9}$$

Note that Eq. (9) relates $P,\tau_0$ and the position of the system, $L_{\tau_0}^{P_0+P}=L_{cr}$ at the instant of release of the force $P$. Also observe that the previously described critical condition depends on the evaluation of two parameters, $P$ and $\tau$. One approach is to prescribe $\tau_0$ and find the corresponding $P_{cr}$ and the other is to prescribe $P$ and find the corresponding $\tau_{0_{cr}}$. The two are equivalent. Regardless of the approach, Eq. (9) relates three parameters, $P$, $\tau_{0_{cr}}$ (or $P_{cr},\tau$), and $L_{cr}$ (the position of the system at the instant of release, taken as one parameter).

The second (needed) equation is obtained from Eq. (4). This equation is used to relate the load $P$, the time of release $\tau_0$, and the position of the system at the instant of release. In order to find, for a prescribed sudden load $P$, the position of the system at the instant of release, one must specify the path of motion. For one-degree-of-freedom systems there is only one path and this is accomplished easily. On the other hand, for a multi-degree-of-freedom system there are numerous possible paths leading to a multitude of positions for a given release time. In such cases, if one is interested in finding a lower bound for the critical condition, the path that yields the smallest possible time must be found. This may be accomplished by solving the proper "brachistochrone" problem. Thus, Eq. (4) along with the path of motion, relates

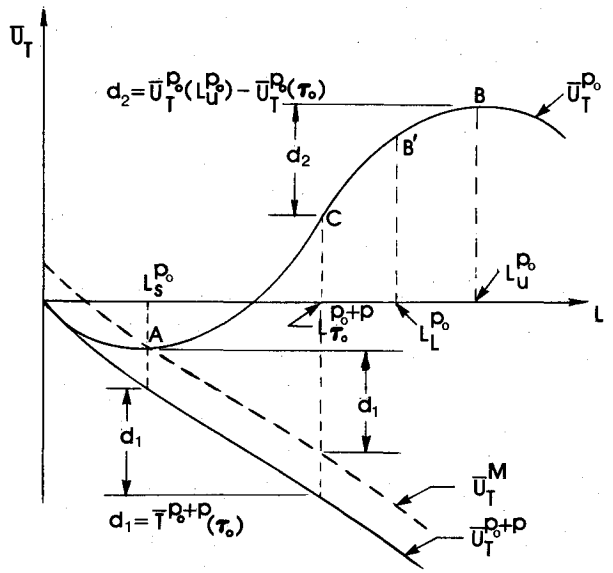


**Fig. 1 Total potential curves.**

the release time $\tau_0$ and the system position at the instant of release.

Finally, in the case for which a critical condition is defined through the existence of a maximum allowable position ($L_L^{P_0}$, see Fig. 1) critical loads can be estimated by following the same procedure. The only difference is that position B is replaced by B′, or $\bar{U}_T^{P_0}(L_u^{P_0})$ is replaced by $\bar{U}_T^{P_0}(L_L^{P_0})$. Such cases can possibly exist in deflection-limited designs.

Parenthetically, the cases of ideal impulse, and suddenly applied load of constant magnitude and infinite duration, may be obtained as special cases of the present procedure. However, critical conditions for these two load cases may also be obtained independently.

For the ideal impluse case, one may relate the impulse to an initial kinetic energy, and, from conservation of energy,

$$\bar{U}_T^{P_0} + \bar{T}^{P_0} = \bar{U}_T^{P_0}(L_S^{P_0}) + \bar{T}_i^{P_0} \tag{10}$$

Then, $\bar{T}_i^{P_0}$ is critical (related to the critical ideal impluse ) if the system reaches position $L_u^{P_0}$ (point B of Fig. 1) with zero kinetic energy. Thus,

$$\bar{T}_{i_{cr}}^{P_0} = \bar{U}_T^{P_0}(L_S^{P_0}) - \bar{U}_T^{P_0}(L_T^{P_0}) \tag{11}$$

For the secod extreme case ($\tau_0 \to \infty$), $P_{cr}$ may be obtained from Eqs. (3) or (4), which for this case holds true for all $\tau(0 \le \tau \le \infty)$. Thus, $P_{cr}$ corresponds to the solution of

$$\bar{U}_T^{P_0+P}(L_u^{P_0+P}) = \bar{U}_T^{P_0+P}(L_S^{P_0}) \tag{12}$$

where $L_u^{P_0+P}$ denotes the unstable static equilibrium position of the system when the static load is equal to $P_0+P$.

Three systems are chosen in order to demonstrate the preceding concepts and the necessary solution technique for obtaining estimates of the critical conditions. The analysis of each system is presented separately.

## Simple Mechanical Model

This model is a one-degree-of-freedom model (see Fig. 2) and is characteristic of imperfection-sensitive configurations, for which the imperfection is a load eccentricity. The complete static stability analysis of this model is presented in Ref. 23, Article 2.5.

The expressions for the nondimensionalized total potential and kinetic energy are

$$\bar{U}_T^P = U_T^P/(\tfrac{1}{2}ka^2) = \sin^2\theta - 2p(1-\cos\theta+\bar{e}\sin\theta) \tag{13}$$

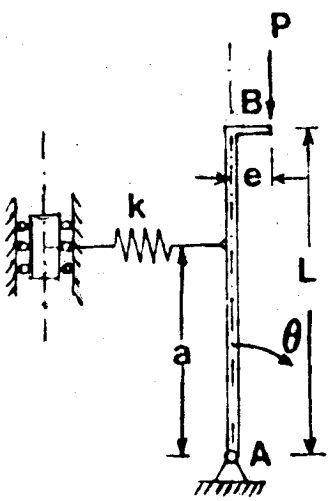


Fig. 2 Geometry of simple mechanical model (one degree of freedom).

and

$$\bar{T}^P = \frac{2T^P}{ka^2} = \frac{1}{2}I\left(\frac{d\theta}{dt}\right)^2 \Big/ \frac{1}{2}ka^2 = \left(\frac{d\theta}{d\tau}\right)^2 \tag{14}$$

where $p = PL/ka^2$, $\bar{e} = e/L$, $\tau = \sqrt{ka^2/I}$, and $I$ is the system moment of inertia about the hinge A (see Fig. 2).

In evaluating the effect of static preloading for this model, three load eccentricities are chosen, and, for each eccentricity, three static preloading load levels $P_0$. These are given next, along with the corresponding static critical load (see Ref. 23). Note, $p_0 < P_{cr_s}$.

$$\bar{e}=0.005;\ p_0=0.35,\ 0.40,\ 0.50;\ p_{cr_s}=0.955$$

$$\bar{e}=0.010;\ p_0=0.30,\ 0.40,\ 0.50;\ p_{cr_s}=0.932$$

$$\bar{e}=0.020;\ p_0=0.30,\ 0.40,\ 0.50;\ p_{cr_s}=0.898$$

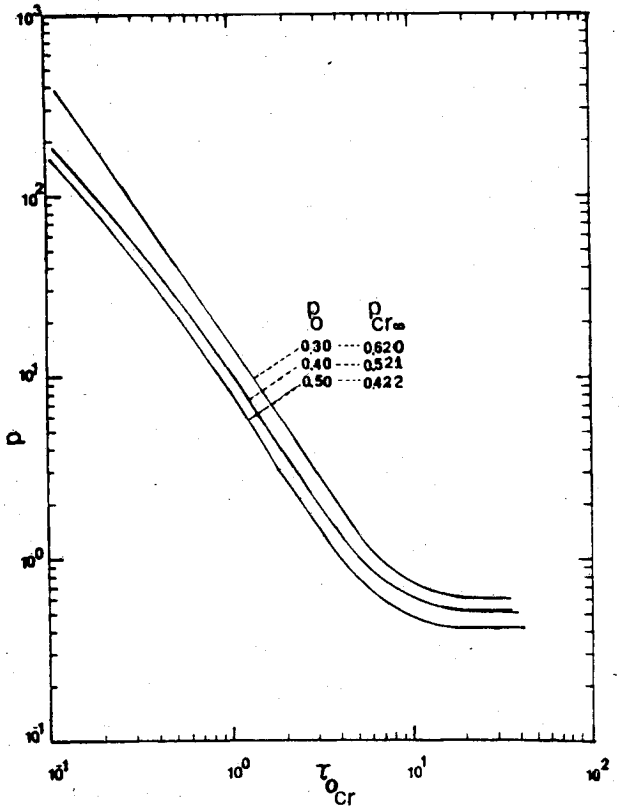


Fig. 3 Critical dynamic conditions (simple mechanical model).

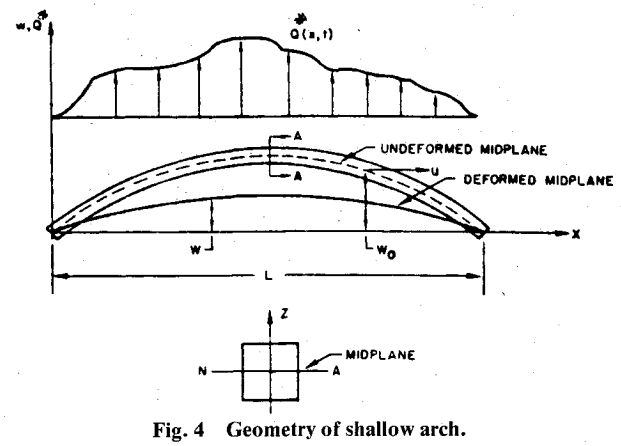


Fig. 4 Geometry of shallow arch.

The following steps are employed, according to the outlined procedure, in order to obtain critical conditions. Note that the system is first loaded statically to a level $p_0$ and, then, suddenly, with a load $p$ applied for $\tau_0$ units of time.

1) For each $p_0$ obtain the corresponding $\theta_s^{P_0}$ and $\theta_u^{P_0}$, from the static stability analysis.

2) Use of Eq. (9), one of the two governing equations for estimating critical conditions, yields

$$2p(\cos\theta_s^{P_0} - \bar{e}\sin\theta_s^{P_0} - \cos\theta_{cr} + \bar{e}\sin\theta_{cr}) = \sin^2\theta_u^{P_0} - \sin^2\theta_s^{P_0}$$

$$-2p_0(\cos\theta_s^{P_0} - \bar{e}\sin\theta_s^{P_0} - \cos\theta_u^{P_0} + \bar{e}\sin\theta_u^{P_0}) \qquad (15)$$

where $\theta_{cr}$ is the position the system has reached at the instant of release of the force $P(\tau = \tau_{0_{cr}})$. Note that in Eq. (15) every parameter is known ($\theta_s^{P_0}$, $\bar{e}$, $\theta_u^{P_0}$, and $p_0$) except $p$ and $\theta_{cr}$.

3) The second governing equation is obtained from Eq. (4). Use of Eqs. (13) and (14) in Eq. (4) yields

$$\tau_{0_{cr}} = \int_{\theta_s^{P_0}}^{\theta_{cr}} \{\sin^2\theta_s^{P_0} - \sin^2\theta - 2(p_0+p)(\bar{e}\sin\theta_s^{P_0} - \cos\theta_s^{P_0}$$

$$-\bar{e}\sin\theta + \cos\theta)\}^{-1/2}\,d\theta \qquad (16)$$

Note that in Eq. (16) all parameters are known, except $p$, $\theta_{cr}$ and $\tau_{0_{cr}}$. A critical condition is characterized by $(p,\tau_0)$ that satisfies Eqs. (15) and (16). This means that for a given release time $\tau_0$, find $p_{cr}$ (and, consequently, $\theta_{cr}$) or for a given $p$ find $\tau_{0_{cr}}$ (and, consequently, $\theta_{cr}$). Computationally though, it is easier to assign values of $\theta_{cr}$, solve for $p$ from Eq. (15) and, then, solve for the corresponding $\tau_{0_{cr}}$ from Eq. (16). A computer program has been written for these computations.

Results for the extreme cases of $\tau_0 \to 0$ (ideal impluse) and $\tau_0 \to \infty$ are presented in tabular form in Tables 1 and 2. Partial results are presented in Fig. 3 for the finite duration case (general case).

## Shallow Arch

Consider a slender arch of small initial curvature and symmetric cross section supported at the ends by immovable supports and loaded transversly by a distributed load (see Fig 4). The undeformed and deformed arch midlines are denoted by $w_0(x)$ and $w(x)$, respectively. The horizontal displacemnt component of material points on the midline are characterized by $u(x)$. The specific goemetry that is employed herein is a half sine, simply supported arch loaded transversely by a half sine distributed load. This configuration has been analyzed in Refs. 9, 12, and 14 for the cases of an ideal impulsive load and of a constant load of infinite duration without static preloading. The case of constant load of finite duration without static preloading can be found in Ref. 12. Finally, the complete static stability analysis is presented in Ref. 23, Article 7.5. The symbols and nondimensionalization are exactly the same as those of Ref. 23.

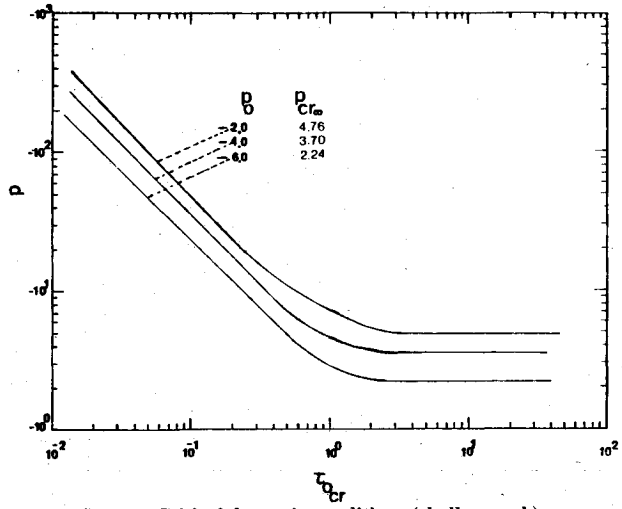


Fig. 5 Critical dynamic conditions (shallow arch).

The relevant nondimensionalized parameters are shown here.

$$\xi = \pi x/L; \quad \eta(\xi) = w(x)/\rho; \quad v(\xi) = u(x)/\rho$$

$$q(\xi) = \frac{\rho Q^*(\xi)}{P_E \epsilon_E L} \qquad p = \frac{P}{P_E} \qquad \bar{U}_T = \frac{4U_T^*}{P_E \epsilon_E L}$$

$$\bar{T} = \frac{4T^*}{P_E \epsilon_E L} \qquad \tau = \frac{\pi t}{L}\sqrt{E\frac{\bar{\epsilon}_E}{\sigma}} \qquad (17)$$

where $\rho^2 = I/A$, $P_E = \pi^2 EI/L^2$, $\bar{\epsilon}_E = (\pi\rho/L)^2$, $P$ is the axial force in the arch, $A$ and $I$ the cross-sectional area and second moment of the area, respectively, $E$ is Young's modulus of elasticity, and $\sigma$ the volume density of the material. In this analysis, the rotatory and in-plane kinetic energies are neglected, thus,

$$T^* = \frac{\sigma A}{2}\int_0^L \left(\frac{\partial w}{\partial t}\right)^2 dx \qquad (18)$$

**Table 1 Critical ideal impulse $(p\tau_0)_{cr}$ (simple mechanical model)**

| $\bar{e}=0.005$ | | $\bar{e}=0.010$ | | $\bar{e}=0.020$ | |
|---|---|---|---|---|---|
| $p_0$ | $(p\tau_0)_{cr}$ | $p_0$ | $(p\tau_0)_{cr}$ | $p_0$ | $(p\tau_0)_{cr}$ |
| 0 | 200 | 0 | 100 | 0 | 50 |
| 0.350 | 192 | 0.300 | 88 | 0.300 | 42 |
| 0.400 | 164 | 0.300 | 76 | 0.400 | 36 |
| 0.500 | 139 | 0.500 | 62 | 0.500 | 29 |
| 0.955 | 0 | 0.932 | 0 | 0.898 | 0 |

**Table 3 Critical ideal impulse $(p\tau_0)_{cr}$ (shallow pinned arch)**

| $e=4.5$ | | $e=5.0$ | | $e=6.0$ | |
|---|---|---|---|---|---|
| $p_0$ | $(p\tau_0)_{cr}$ | $p_0$ | $(p\tau_0)_{cr}$ | $p_0$ | $(p\tau_0)_{cr}$ |
| 0 | −8.71 | 0 | −10.06 | 0 | −12.64 |
| −1.0 | −5.11 | −2.0 | −4.95 | −3.00 | −7.95 |
| −3.0 | −3.53 | −4.0 | −3.64 | −4.00 | −6.80 |
| −5.0 | −1.93 | −6.0 | −2.28 | −6.00 | −5.31 |
| −6.3 | 0 | −9.0 | 0 | −13.42 | 0 |

**Table 2 Critical dynamic loads for $\tau_0 \to \infty$, $p_{cr_\infty}$ (simple mechanical model)**

| $\bar{e}=0.005$ | | | $\bar{e}=0.010$ | | | $\bar{e}=0.020$ | | |
|---|---|---|---|---|---|---|---|---|
| $p_0$ | $p_{cr_\infty}$ | $p_0+p_{cr_\infty}$ | $p_0$ | $p_{cr_\infty}$ | $p_0+p_{cr_\infty}$ | $p_0$ | $p_{cr_\infty}$ | $p_0+p_{cr_\infty}$ |
| 0 | 0.948 | 0.948 | 0 | 0.912 | 0.912 | 0 | 0.850 | 0.850 |
| 0.350 | 0.601 | 0.951 | 0.300 | 0.620 | 0.920 | 0.300 | 0.570 | 0.870 |
| 0.400 | 0.552 | 0.952 | 0.400 | 0.521 | 0.921 | 0.400 | 0.477 | 0.877 |
| 0.500 | 0.453 | 0.953 | 0.500 | 0.422 | 0.922 | 0.500 | 0.381 | 0.881 |
| 0.955 | 0 | 0.955 | 0.932 | 0 | 0.932 | 0.898 | 0 | 0.898 |

**Table 4 Critical dynamic loads for $\tau_0 \to \infty$, $p_{cr_\infty}$ (shallow pinned arch)**

| | $e=4.5$ | | | $e=5.0$ | | | $e=6.0$ | |
|---|---|---|---|---|---|---|---|---|
| $p_0$ | $p_{cr_\infty}$ | $p_0+p_{cr_\infty}$ | $p_0$ | $p_{cr_\infty}$ | $p_0+p_{cr_\infty}$ | $p_0$ | $p_{cr_\infty}$ | $p_0+p_{cr_\infty}$ |
| 0 | −3.70 | −3.70 | 0 | −5.20 | −5.20 | 0 | −8.20 | −8.20 |
| −1.00 | −3.35 | −4.35 | −2.0 | −4.76 | −6.76 | −3.00 | −7.71 | −10.71 |
| −3.00 | −2.54 | −5.54 | −4.0 | −3.70 | −7.70 | −4.00 | −7.21 | −11.22 |
| −5.00 | −0.99 | −5.99 | −6.0 | −2.24 | −8.24 | −6.00 | −6.37 | −12.37 |
| −6.30 | 0 | −6.30 | −9.0 | 0 | −9.00 | −13.42 | 0 | −13.42 |

**Table 5 Imperfection parameters and static critical load**

| Wavenumbers | | | | | |
|---|---|---|---|---|---|
| Asymmetrical, $k$ | Axisymetrical, $i$ | Circular, $l$ | Imperfection parameters $\bar{\xi}_2$ | $\bar{\xi}_1$ | Critical load, $\lambda_s$ |
| 1 | 2 | 9 | 0.1754 | −0.1130 | 0.8765 |
| 2 | 4 | 13 | 0.0534 | −0.0499 | 0.8962 |
| 4 | 8 | 18 | 0.0172 | −0.0220 | 0.9173 |
| 6 | 12 | 21 | 0.0093 | −0.0136 | 0.9254 |
| 8 | 16 | 24 | 0.0058 | −0.0097 | 0.9263 |
| 10 | 20 | 26 | 0.0042 | −0.0075 | 0.9226 |
| 12 | 24 | 27 | 0.0033 | −0.0060 | 0.9120 |
| 14 | 28 | 28 | 0.0027 | −0.0050 | 0.8970 |
| 16 | 32 | 29 | 0.0022 | −0.0043 | 0.8838 |
| 18 | 36 | 29 | 0.0020 | −0.0037 | 0.8831 |

For the specific geometry and loading considered here one may write

$$\eta_0(\xi) = e\sin\xi \quad \text{and} \quad q(\xi,\tau) = q_1(\tau)\sin\xi \tag{19}$$

where $e$ is the initial rise parameter.

Following the solution procedure of Refs. 9 and 12, the response of the arch $\eta(\xi,\tau)$ is represented by

$$\eta(\xi,\tau) = \eta_0(\xi) + a_1(\tau)\sin\xi + a_2(\tau)\sin 2\xi \tag{20}$$

A more convenient set of equations is obtained by introducing two new parameters (as in Refs. 9 and 12)

$$r = a_1 + e \qquad p = q_1 + e \tag{21}$$

With these nondimensionalized parameters, the expressions for the total potential and kinetic energy are ($\bar{U}_T = \bar{U}_T^P$)

$$\bar{U}_T^P = \tfrac{1}{8}(r^2 - e^2 + 4a_2^2)^2 + r^2 - e^2 + 16a_2^2 + 2p(e-r) \tag{22}$$

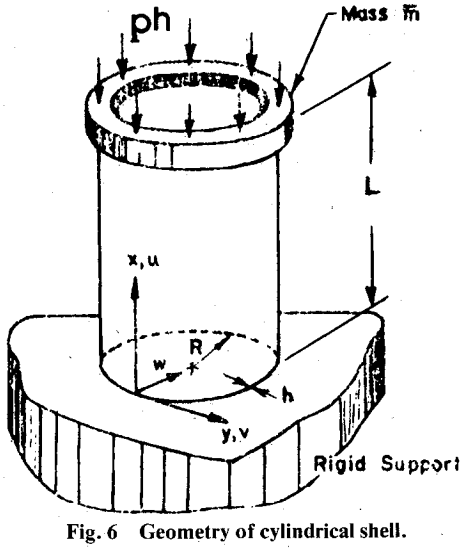


Fig. 6 Geometry of cylindrical shell.

$$\bar{T}^P = \frac{2}{\pi}\int_0^\pi \left(\frac{d\eta}{d\tau}\right)^2 \qquad d\xi = \left(\frac{dr}{d\tau}\right)^2 + \left(\frac{da_2}{d\tau}\right)^2 \tag{23}$$

Note that this special geometry problem has been reduced to that of a two-degree-of-freedom system $(r,a_2)$. Furthermore, the static stability analysis reveals that for $e>4$ the total potential possesses five equilibrium positions, two stable positions (relative minimums, one near and one far) and three unstable positions (one relative maximum and two saddle points). Because of this, by employing the approaches of Refs. 9, 12, and 14, critical conditions, under sudden application of the load, can only be bracketed between a lower bound (termed minimum possible critical load by Simitses[12] and sufficient condition for stability by Hsu[14]) and an upper bound (termed minimum guaranteed critical load by Simitses and sufficient condition for instability by Hsu). In this paper, only the lower bound is estimated. Moreover, for the case of finite duration, knowledge of the path of motion is required in order to evaluate the critical duration time $\tau_{0_{cr}}$ for a given value of the load $p$. Since the path initially is symmetric ($a_2 \equiv 0$), it is assumed that the path is indeed symmetric for all duration times (for computational convenience).

Under these assumptions the necessary steps are given as follows.

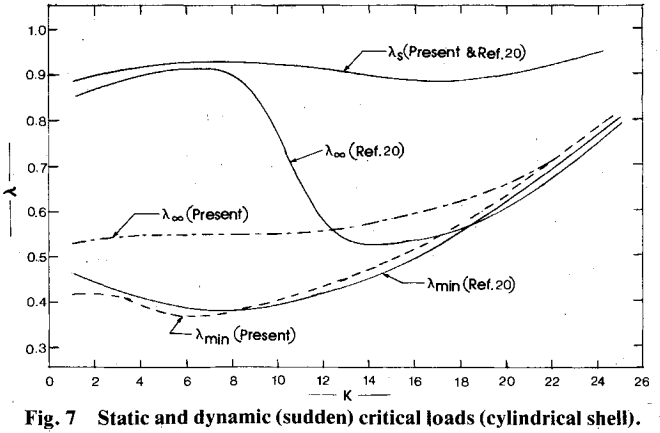


Fig. 7 Static and dynamic (sudden) critical loads (cylindrical shell).

1) Through a static stability analysis, establish the unstable position with the smallest value for the total potential $L_u^{P_0}$ for each $p_0$ value (level of static preloading). For this case, the total potential at a saddle point (unstable) is lower than that at the relative maximum unstable point.

$L_u^{P_0}$ is characterized by (saddle point)

$$r=p_0/3 \qquad a_2^2=\tfrac{1}{4}(e^2-16-p_0/9) \tag{24}$$

Also establish the near stable static equilibrium position $P_s^{P_0}$. This position is characterized by $a_2\equiv 0$ and an $r$ value obtained from the following cubic:

$$r^3-(e^2-4)r=4p_0 \tag{25}$$

For more details on the static analysis see Ref. 23.

2) Use of Eq. (9) yields

$$2p(r_{cr}-r_s^{P_0})=-32+\frac{p_0^2}{3}+4e^2-\frac{1}{8}[(r_s^{P_0})^2-e^2]^2$$

$$-(r_s^{P_0})^2+2p_0(r_s^{P_0}) \tag{26}$$

Note that in Eq. (26) only $p$ and $r_{cr}$ are unknown parameters.

3) If the path is assumed symmetric, then from Eq. (23)

$$\bar{T}=\left(\frac{dr}{d\tau}\right)^2 \tag{27}$$

and from Eq. (4), the second governing equation becomes

$$\tau_{0_{cr}}=\int_{r_s}^{r_{cr}}P_0[\tfrac{1}{8}\{(r_s^{P_0})^2-e^2\}^2+(r_s^{P_0})^2-r^2$$

$$-\tfrac{1}{2}(r^2-e^2)^2+2(p+p_0)(r-r_s^{P_0})]^{-\frac{1}{2}}dr \tag{28}$$

Note that, for this system, it is more convenient (computationally) to assign values of $r_{cr}$ ($=r_s^{P_0}-\delta r$; starting with a very small value for $\delta r$ and continuously increasing it), solve Eq. (26) for $p$, and then Eq. (28) for $\tau_{0_{cr}}$.

Results are generated for three values of rise parameter $e$, and three values of preloading $p_0$, for each $e$ value. These are

$e=4.5$; $p_0=$ 1.0, −3.0, −5.0; $p_{cr_s}=-6.30$

$e=5.0$; $p_0=-2.0, -4.0, -6.0$; $p_{cr_s}=-9.00$

$e=6.0$; $p_0=-3.0, -4.0, -6.0$; $p_{cr_s}=-13.416$

The results are presented in tabular form for the extreme cases of $\tau\to 0$ and $\tau_0\to\infty$ (see Tables 3 and 4) and graphically, in part, for the finite duration case (see Fig. 5).

## Imperfect Thin Cylindrical Shell

The geometry and load condition chosen are the same as those used by Tamara and Babcock[20] in their dynamic analysis. Because of the complexity of the problem, for this particular application, only the extreme case of $\tau_0\to\infty$ is considered. First, critical conditions without static preloading are obtained and compared to the results of Ref. 20. Then, results are generated in order to study the effect of static preloading.

In their analysis, Tamara and Babcock[20] studied the dynamic buckling (suddenly applied axial load with infinite duration) of an imperfect thin circular cylindrical shell. Their analysis includes the effect of axial inertia and of a mass on the loaded edge of the shell. Moreover, they present results for $L/R=2$ and $R/t=1000$ and various values of the initial imperfection, which are experimentally obtained. Their dynamic response of the shell is based on a four degree-of-freedom representation, and it is obtained from an extensive study of the static behavior. Finally, in order to obtain critical conditions, they employ the Budiansky-Roth[10] criterion. For more detail see Refs. 20 and 24.

The geometry of the shell, taken from Refs. 20 and 24, is shown on Fig. 6. The approximate shell response (displacement components) is also taken from these references.

$$w(x,y,t)=h\left[\xi_1(t)\cos\frac{i\pi x}{L}+\xi_2(t)\sin\frac{k\pi x}{L}\sin\frac{ly}{R}+\xi_3(t)\right]$$

$$u(x,y,t)=u_p(x,y,t)-\xi_0(t)(x/L)h$$

$$v(x,y,t)=v_p(x,y,t) \tag{29}$$

The initial imperfections, on the other hand, are

$$\bar{w}(x,y)=h\left[\bar{\xi}_1\cos\frac{i\pi x}{L}+\bar{\xi}_2\sin\frac{k\pi x}{L}\sin\frac{ly}{R}\right] \tag{30}$$

where $h$ is the shell thickness, $L$ the shell length, $R$ the shell radius, $i$, $k$, and $l$ integers, $u_p$ and $v_p$ particular solutions obtained in terms of known parameters (see Ref. 24), and $\xi_j(t)$, $j=0, 1, 2,$ and 3 denote the four degrees of freedom.

The expression for the total potential $U_T^P$ is given by (from Ref. 24)

$$U_T^P=(\pi Eh^3L/R)[\hat{C}_1(\xi_2^2+2\bar{\xi}_2\xi_2)^2+\hat{C}_2(\xi_1\xi_2+\bar{\xi}_1\xi_2+\bar{\xi}_2\xi_1)^2$$

$$+\hat{C}_3\xi_2^2+\tfrac{1}{2}\xi_1^2+\{\bar{g}_x(\xi)\}^2+\{g_y(\xi)\}^2+2\nu\bar{g}_x(\xi)\bar{g}_y(\xi)$$

$$+\Omega_1\xi_1(\xi_2^2+2\bar{\xi}_2\xi_2)+\Omega_2\xi_2(\xi_1\xi_2+\bar{\xi}_1\xi_2+\bar{\xi}_2\xi_1)$$

$$+\hat{C}_4\xi_1^2+\hat{C}_5\xi_2^2-(2R/L)\bar{p}\xi_0] \tag{31}$$

where $\bar{g}_x$, $\bar{g}_y$, $\hat{C}_i$, and $\Omega_i$ can be found in Ref.24,

$$\bar{p}=PR/Eh \tag{32}$$

and $P$ is the uniform stress applied at the free end of the shell (see Fig. 6). Finally, according to Ref. 24, for the static analysis the three wavenumbers $i$, $k$, and $l$, as well as the two initial imperfection parameters $\bar{\xi}_1$, $\bar{\xi}_2$ are not free, but must satisfy certain relations. The results of this and the corresponding static critical load, $\lambda_s$ ($=P_{cr}/\sigma_{cl}$; where

**Table 6 Critical dynamic conditions for a statically preloaded cylindrical shell**

| | $k=2$ | | | $k=6$ | | | $k=10$ | |
|---|---|---|---|---|---|---|---|---|
| $\lambda_0$ | $\lambda_\infty$ | $\lambda_0+\lambda_\infty$ | $\lambda_0$ | $\lambda_\infty$ | $\lambda_0+\lambda_\infty$ | $\lambda_0$ | $\lambda_\infty$ | $\lambda_0+\lambda_\infty$ |
| 0 | 0.530 | 0.530 | 0 | 0.548 | 0.548 | 0 | 0.555 | 0.555 |
| 0.200 | 0.480 | 0.680 | 0.200 | 0.512 | 0.712 | 0.200 | 0.510 | 0.710 |
| 0.400 | 0.390 | 0.790 | 0.400 | 0.417 | 0.817 | 0.400 | 0.411 | 0.811 |
| 0.600 | 0.252 | 0.852 | 0.600 | 0.280 | 0.880 | 0.600 | 0.278 | 0.878 |
| 0.896 | 0 | 0.896 | 0.925 | 0 | 0.925 | 0.922 | 0 | 0.922 |

$\sigma_{cl} = Eh/[R\sqrt{3(1-\nu^2)}]$), as computed by Tamura,[24] are shown on Table 1 of Ref. 24. Part of this table is shown here as Table 5.

For this particular illustration, critical dynamic conditions are obtained through Eq. (12). First, the total potential, Eq. (31), is nondimensionalized

$$\bar{U}_T^p = U_T^p/(\pi E h^3 L/R) \tag{33}$$

Next, the total potential is modified such that there are no terms that depend entirely on $\bar{p}$,

$$\bar{U}_{T_{\text{mod}}}^p = \bar{U}_T^p + (1-\nu^2)\bar{p}^2 \tag{34}$$

Note that according to the principle of conservation of energy $U_T + T = C$. In the absence of initial kinetic energy, at $\xi_1 = \xi_2 = \xi_3 = 0$, the constant is $\bar{p}$ independent, or

$$C = -(1-\nu^2)\bar{p}^2 \tag{35}$$

By modifying the total potential, the conservation equation becomes $\bar{U}_{T_{\text{mod}}}^p + \bar{T} = 0$. Another point of view is that the $\bar{p}$-only dependent part of the total potential is associated with the part of $\xi_0$, which is independent of $\xi_i$ ($i = 1,2,3$).

Note that from the static equilibrium equation of Ref. 24, one can write

$$\xi_0 = (1-\nu^2)(L/R)\bar{p} + f(\xi_1, \xi_2, \xi_3) \tag{36}$$

Then, if instability is to occur under sudden application of the load, it should not be expected to occur through the mode $\xi_0 = (1-\nu^2)(L/R)\bar{p}$, but only through the existence of $\xi_1(t)$, $\xi_2(t)$, and $\xi_3(t)$.

Then, through a static stability analysis, one can solve for all the static equilibrium points. This was done independently (from Ref. 24 ) and the static critical loads agree well with those of Tamura[24] (see Fig. 7). Furthermore, dynamic critical loads are computed from Eq. (12) with zero static preloading and are compared with those of Tamura[24] corresponding to the case of $\bar{m} = 0$ (neglecting in-plane inertia) in Fig. 7. On this same figure, minimum post-limit point loads are also plotted vs the asymmetric wavenumber $k$.

Finally, through Eq (12), critical conditions for statically preloaded shells are obtained. These are shown on Table 6, for three $k$ values and several values of static loading $\lambda_0$.

## Conclusions

Concepts of dynamic instability of statically preloaded systems, subjected to sudden loads of finite duration, have been presented. Moreover, criteria of dynamic instability and estimates of critical conditions have been discussed. Finally, these have been demonstrated through simple structural configurations.

Note that the estimates represent true critical conditions for one-degree-of-freedom systems. On the other hand, for multi-degree-of-freedom systems, the estimates represent lower bounds for critical dynamic conditions. [Minimum Possible Critical Load (MPCL) according to Ref. 12 and sufficiency conditions for stability according to Hsu.[13-17]] One important result is that the effect of static preloading seems to be the same regardless of the particular model. Specifically, 1) for the extreme case of the ideal impulse, the critical impulse decreases with increasing values of static preloading; and 2) similarly, for the other extreme case (constant load of infinite duration), the total load (static preload plus critical dynamic load) increases with increasing values of static preloading. Both of these observations are very significant in the design of dynamically loaded systems, because the "zero static preloading" analyses are much simpler in execution, but yet they provide a limiting behavior under static preloading (at a level below the static critical load).

## Acknowledgments

This work was partially supported by the USAF, Aeronautical Systems Division (AFSC), Wright-Patterson Air Force Base. The financial support provided by the United States Air Force is gratefully acknowledged. Thanks are also extended to Dein Shaw for providing assistance in the preparation of the manuscript.

## References

[1] Bolotin, V. V., *The Dynamic Stability of Elastic Systems,* translated by V. I. Weingarter, L. B. Greszczuk, K. N. Trirogoff, and K. D. Gallegos, Holden Day, San Francisco, 1964.

[2] Bolotin, V. V., *Nonconservative Problems of the Theory of Elastic Stability,* Moscow 1961; English translation by T. K. Lusher, Pergamon Press, New York, 1963.

[3] Herrmann, G., "Stability of Equilibrium of Elastic Systems Subjected to Nonconservative Forces," *Applied Mechanics Reviews,* Vol. 20, No. 2, 1967, pp. 103-108.

[4] Stoker, J. J., "On the Stability of Mechanical Systems," *Communication of Pure and Applied Math.,* Vol. VIII, 1955, pp. 133-142.

[5] Seckel, E., *Stability and Control of Airplanes and Helicopters,* Academic Press, New York, 1964.

[6] Lefschetz, S., *Stability of Nonlinear Control Systems,* Academic Press, New York, 1965.

[7] Paidoussis, M. P., "Dynamics of Tubular Cantilevers Conveying Fluid," *Journal of Mechanical Engineering Science,* Vol. 42, No. 2, 1970, pp. 85-103.

[8] Bohn, M. P. and Herrmann, G., "Instabilities of a Spatial System of Articulated Pipes Conveying Fluid," *Journal of Fluid Engineering,* Vol. 41, No. 1, 1974, pp. 289-296.

[9] Hoff, N. J. and Bruck, V. G., "Dynamic Analysis of the Buckling of Laterally Loaded Flat Arches," *Journal of Mathematics and Physics,* Vol. 32, No. 4, 1954, pp. 276-288.

[10] Budiansky, B. and Roth, R. S., "Axisymmetric Dynamic Buckling of Clamped Shallow Spherical Shells," Collected Papers on Instability of Shell Structures, NASA TN D-1510, Aug. 1962,

[11] Budiansky, B. and Hutchinson, J. W., "Dynamic Buckling of Imperfection-Sensitive Structures," *Proceedings of XI International Congress of Applied Mechanics,* Munich, 1964.

[12] Simitses, G. J., "Dynamic Snap-Through Buckling of Low Arches and Shallow Caps," Ph.D. Dissertation, Department of Aeronautics and Astronautics, Stanford University, Stanford, Calif., June 1965.

[13] Hsu, C. S., "On Dynamic Stability of Elastic Bodies with Prescribed Initial Conditions," *International Journal of Engineering Sciences,* Vol. 4, 1966, pp. 1-21.

[14] Hsu, C. S., "The Effects of Various Parameters on the Dynamic Stability of a Shallow Arch," *Journal of Applied Mechanics,* Vol. 34, No. 2, 1967, pp. 349-356.

[15] Hsu, C. S., "Stability of Shallow Arches Against Snap-Through Under Timewise Step Loads," *Journal of Applied Mechanics,* Vol. 25, No. 1, 1968, pp. 31-39.

[16] Hsu, C. W., "Equilibrium Configurations of a Shallow Arch of Arbitrary Shape and their Dynamic Stability Character," *International Journal of Nonlinear Mechanics,* Vol. 3, June 1968, pp. 113-136.

[17] Hsu, C. S., Huo, C. T., and Lee, S. S., "On the Final States of Shallow Arches on Elastic Foundations Subjected to Dynamic Loads," *Journal of Applied Mechanics,* Vol. 35, No. 4, 1968, pp. 713-723.

[18] Budiansky, B., "Dynamic Buckling of Elastic Structures: Criterion and Estimates," *Dynamic Stability of Structures,* edited by G. Herman, Pergamon Press, 1967, pp. 83-108.

[19] Simitses, G. J., "On the Dynamic Buckling of Shallow Spherical Caps," *Journal of Applied Mechanics,* Vol. 41, No. 1, 1974, pp. 299-300.

[20] Tamura, Y. S. and Babcock, C. D., "Dynamic Stability of Cylindrical Shells Under Step Loading," *Journal of Applied Mechanics,* Vol. 42, Ser. E, March 1975, pp. 190-194.

[21] Zimcik, D. G. and Tennyson, R. C., "Stability of Circular Cylindrical Shells Under Transient Axial Impulsive Loading," *Proceedings AIAA/ASCE/AHS 20th Structures, Structural Dynamics and Materials Conference,* St. Louis, Mo., April 4-6, 1979.

[22] Simitses, G. J., "Dynamic Stability of Structural Elements Subjected to Step-Loads," *Proceedings, Army Symposium on Solid Mechanics, 1980;* Designing for Extremes: Environment, Loading, and Structural Behavior, South Yarmouth, Cape Cod, Mass., Sept. 30-Oct. 2, 1980, pp. 87-107.

[23] Simitses, G. J., *Elastic Stability of Structures,* Prentice-Hall, Inc., Englewood Cliffs, N. J., 1976.

[24] Tamura, Y. S., "Dynamics Stability of Cylindrical Shells under Step Loading," AFOSR TR-74-0460 (AD-777 291), prepared for AFOSR under Grant 73-2447, California Institute of Technology, Pasadena, Calif., 1973.